THE JOURNAL OF BIOLOGICAL CHEMISTRY VOL. 287, NO. 24, pp. 19904–19915, June 8, 2012

Caveolin-1 and Dynamin-2 Are Essential for Removal of the Complement C5b-9 Complex via Endocytosis*[S]

Received for publication, December 12, 2011, and in revised form, April 18, 2012 Published, JBC Papers in Press, April 23, 2012, DOI 10.1074/jbc.M111.333039

Oren Moskovich[‡], Lee-Or Herzog[‡], Marcelo Ehrlich[§], and Zvi Fishelson[‡1]

From the [‡]Departments of Cell and Developmental Biology, Sackler School of Medicine and [§]Cell Research and Immunology, George S. Wise Faculty of Life Sciences, Tel Aviv University, Tel Aviv 69978, Israel

Background: Cells resist complement-dependent cytotoxicity by elimination of the membranolytic C5b-9 complex from their surface.
Results: Modulations of caveolin-1 and dynamin-2 expression and activity affect C5b-9 endocytosis and cell death.
Conclusion: Elimintion of C5b-9 and complement resistance depend on caveolae formation, dynamin activity and lipid rafts.
Significance: Targeting of key factors in the C5b-9 elimination pathway may enable us to regulate C5b-9 homeostasis and cell resistance to complement-dependent cytotoxicity.

The complement system, an important element of both innate and adaptive immunity, is executing complement-dependent cytotoxicity (CDC) with its C5b-9 protein complex that is assembled on cell surfaces and transmits to the cell death signals. In turn, cells, and in particular cancer cells, protect themselves from CDC in various ways. Thus, cells actively remove the C5b-9 complexes from their plasma membrane by endocytosis. Inhibition of clathrin by transfection with shRNA or of EPS-15 with a dominant negative plasmid had no effect on C5b-9 endocytosis and on cell death. In contrast, inhibition of caveolin-1 (Cav-1) by transfection with an shRNA or a dominant negative plasmid sensitized cells to CDC and inhibited C5b-9 endocytosis. Similarly, both inhibition of dynamin-2 by transfection with a dominant negative plasmid or by treatment with Dynasore reduced C5b-9 endocytosis and enhanced CDC. C5b-9 endocytosis was also disrupted by pretreatment of the cells with methyl-β-cyclodextrin or Filipin III, hence implicating membrane cholesterol in the process. Analyses by confocal microscopy demonstrated co-localization of Cav-1-EGFP with C5b-9 at the plasma membrane, in early endosomes, at the endocytic recycling compartment and in secreted vesicles. Further investigation of the process of C5b-9 removal by exo-vesiculation demonstrated that inhibition of Cav-1 and cholesterol depletion abrogated C5b-9 exo-vesiculation, whereas, over-expression of Cav-1 increased C5b-9 exo-vesiculation. Our results show that Cav-1 and dynamin-2 (but not clathrin) support cell resistance to CDC, probably by facilitating purging of the C5b-9 complexes by endocytosis and exo-vesiculation.

The complement system is an essential effector arm of innate immunity and a regulator of adaptive immunity (1, 2). Following activation of its classical, lectin, or alternative initiation pathway, the common complement terminal pathway generates the membrane attack complex (MAC)[2] composed of the proteins C5b, C6, C7, C8, and C9 (C5b-9 or MAC) (3). The assembled MAC contains a C9 homo-polymer that adheres to and then inserts into the target cell membrane, eventually causing a massive membrane damage, leading to cell swelling and necrotic cell death (4–6). Cell death is inflicted by various toxic moieties activated by the MAC, including elevated concentrations of calcium ions and oxygen radicals, and is amplified by activated JNK and Bid (7, 8). Opposingly, cells remove the MAC from their plasma membrane via endocytosis or exo-vesiculation (9–12) and defy MAC-induced death in various additional ways (13–15). Elimination of the MAC by endocytosis has been demonstrated in several normal and tumor cells (16–18). Pilzer and Fishelson proposed a role for mortalin, the mitochondrial heat shock protein 70, in MAC removal (19, 20).

Eukaryotic cells use the endocytotic process to internalize segments of plasma membrane, cell-surface receptors and various soluble molecules from the extracellular mileu (21). Endocytosis can be mediated by clathrin or caveolin or is independent of them. Ligand binding to membrane receptors may accelerate their interaction with clathrin (present in clathrin-coated pits) through adaptors, such as adaptor protein-2 (AP-2) or epidermal growth factor receptor substrate 15 (EPS-15) (22). Clathrin then polymerizes and enforces invagination of the pit, which is eventually released into the cytoplasm through the action of the large GTPase dynamin (23). Dynamin is also involved in a clathrin-independent endocytic pathway that is regulated by caveolin (24, 25). Caveolae are flask-shaped 50–100 nm invaginations of the plasma membrane, enriched in caveolins, cavins, sphingolipids, and cholesterol (26–28). Caveolae, which are specialized forms of lipid rafts, participate in

* This research was in part supported by grants from the Israel Science Foundation and the Israel Cancer Association.
[S] This article contains supplemental Figs. S1–S8.
[1] To whom correspondence should be addressed: Department of Cell and Developmental Biology, Sackler School of Medicine, Tel Aviv University, Tel Aviv 69978, Israel. Tel.: 972-3-6409620; Fax: 972-3-6407432; E-mail: lifish@post.tau.ac.il.

[2] The abbreviations used are: MAC, complement membrane attack complex; A.U., arbitrary units; C5b-9, complement terminal complex composed of C5b, C6, C7, C8 and C9; C9-AF488, human complement C9 tagged with Alexa Fluor 488; C9-AF555, human complement C9 tagged with Alexa Fluor 555; C9D, C9 depleted; Cav-1, caveolin-1; CDC, complement-dependent cytotoxicity; Dyn-2, dynamin-2; HI, heat inactivated; MβCD, methyl-β-cyclodextrin; MFI, mean fluorescence intensity; NHS, normal human serum.

diverse cellular functions, including endocytosis, calcium signaling, vesicular transport, and cholesterol homeostasis (26, 27). The major scaffold protein of caveolae in the plasma membrane is caveolin-1 (Cav-1) (29, 30). Mammalian cells express two other isoforms of caveolin (Cav-2 and Cav-3) with Cav-3 being muscle specific (26, 27). While Cav-1 and Cav-3 are predominantly expressed in the plasma membrane, Cav-2 is localized in the Golgi apparatus and is targeted to the cell surface and caveolae only upon formation of hetero-oligomers with Cav-1 (31). Among the proteins sequestered within caveolae through interaction with Cav-1, are G protein receptors, Gα subunits, tyrosine kinases, GTPases, and others (26, 27).

Our earlier results demonstrated that C5b-9 is either rapidly shed by ectocytosis directly from the plasma membrane, in membrane vesicles, or is endocytosed, accumulates in the endocytic recycling compartment (ERC), and is to some extent by exocytosis (32). For an insight into the mechanism of MAC endocytosis in K562 erythroleukemia cells, we blocked the clathrin- or caveolin-endocytic pathways and examined MAC removal and sensitivity to cell death. As shown here, endocytosis of the C5b-9 complexes depends on caveolin-1 and dynamin-2 activity and is essential for cell protection from MAC-mediated cell death. Furthermore, cholesterol is indispensable for MAC endocytosis and complement resistance implicating the cholesterol-rich caveolae in these activities.

EXPERIMENTAL PROCEDURES

Sera, Antibodies, and Reagents—Normal human serum (NHS), used as a source for complement, was prepared from healthy individuals. Heat-inactivated NHS (HIS) was prepared by heating NHS for 30 min at 56 °C. C8-deficient human serum (C8D) was prepared from a C8-deficient patient as described (33). Purified human C8, C9, and complement C9-depleted human serum (C9D-NHS) were purchased from Complement Technology Inc (Tyler, TX). Polyclonal antiserum directed to K562 human cells were prepared in rabbits or mice and polyclonal anti-human C3 antibodies were prepared in goats. The chimeric monoclonal antibody against CD20, Rituximab, was purchased from Roche (Basel, Switzerland). Mouse monoclonal antibody directed to a neoepitope in human C5b-9 (clone aE11) was purchased from Diatec Monoclonals (Oslo, Norway). Mouse monoclonal antibody directed to human C9 (clone X197) was purchased from Hycult Biotechnology (Uden, Netherlands). Anti-clathrin heavy chain (clone X22) was from Affinity BioReagents (Golden, CO), anti-human caveolin-1 (clone N-20) was from Santa Cruz Biotechnology (Santa Cruz, CA) and mouse anti-actin antibody was from Chemicon (Temecula, CA). FITC-conjugated goat anti-mouse Fab, FITC-conjugated donkey anti-goat Fab, Cy3-conjugated goat anti-mouse Fab, peroxidase-conjugated goat anti-rabbit IgG and goat anti-mouse IgG were purchased from Jackson Immunoresearch (West Grove, PA). Methyl-β-cyclodextrin (MβCD), cholesterol, Filipin III, Dynasore, streptolysin O (SLO), Hepes, BSA and HBSS were purchased from Sigma (Rehovot, Israel). Transferrin Texas Red-conjugated and Alexa Fluor protein labeling kits were from Molecular Probes.

Plasmids and Transient Transfections—Dynamin-2 mutant plasmid (K44A-EGFP), epidermal growth factor receptor substrate 15 mutant plasmid (DN-EPS15-GFP), shRNA (small-hairpin RNA) against the clathrin-heavy chain (CHC) and scrambled shRNA were previously described (34), (35). shRNA against Caveolin-1 and scrambled shRNA were kindly provided by Dr. Maria Shatz (NIEHS, North Carolina). Cav-1-EGFP and Cav-1 mutant (Cav-1-DGI) plasmids were described (36). For transient transfection, K562 cells (10^7) were transferred to a sterile 0.4 cm electroporation cuvette (Cell Projects, Kent, UK) and electroporated (250 V, 1500 μF) in the presence of 5–30 μg of plasmid. Cells were immediately re-plated in tissue culture dishes (Corning, NY) containing growth medium.

The clathrin heavy chain shRNA oligonucleotide sequence was: 5′-GATCCCC**TGAGCTGTTTGAAGAAGCA**TTCA-AGAGA**TGCTTCTTCAAACAGCTCA**TTTTTA-3′. The Caveolin-1 shRNA oligonucleotide sequence was: 5′-GATCC-CC**ACCAGAAGGGACACACAGT**TTCAAGAGA**ACTGT-GTGTCCCTTCTGGT**TTTTT-3′. In both cases, sequence and vector (pSUPER retro puro) were digested with BglII and HindIII.

Cell Culture, Cell Lysis, and Preparation of Cell Extracts—K562, a human erythroleukemic cell line or Raji, a human B-cell lymphoma line, was cultured in RPMI 1640 supplemented with 10% (v/v) heat-inactivated fetal bovine serum (Invitrogen Laboratories, Grand Island, NY), 2 mM glutamine, 2 mM pyruvate, and antibiotics mixture (Bio-Lab). Cytotoxicity assays were performed as described before (37). Briefly, K562 or Raji cells in duplicates were incubated with different concentrations of anti-K562 antiserum or Rituximab, respectively, for 30 min at 4 °C and then with complement (NHS, C9D-NHS or heat-inactivated (HIS) sera, final: 50%) for 60 min at 37 °C. Cell lysis was determined by trypan blue uptake. Each experiment was performed at least 4 times. Variation in antibody and NHS batches is leading to small variation in extent of cell lysis between experiments. To prepare cell extracts, 40×10^6 cells were mixed with 1 ml of lysis buffer composed of 100 mM Tris, pH 7.5, 10 mM EDTA, protease inhibitor mixture (Sigma) and 1% Triton-X100. After 3 cycles of freezing and thawing, the cell extract was subjected to centrifugation for 15 min at 14,000 $\times$ *g* and the supernatant was collected and diluted with 1 ml of HBSS.

Collection of Secreted Vesicles and Protein Analysis—For collection of secreted vesicles, cells were treated with antibodies for 30 min at 4 °C and then with NHS or HIS (50%) for 10 min at 37 °C. Then, they were extensively washed resuspended in HBSS and incubated at 37 °C. At different time points, cells were removed by centrifugation at 250 $\times$ *g* and supernatants were sedimented first at 5,000 $\times$ *g* to remove cell debris. Then they were subjected to centrifugation at 100,000 $\times$ *g*, for collection of small membrane vesicles. Protein concentration was determined with the BCA Protein Assay kit (Pierce). Protein (20 μg) was subjected to SDS-PAGE under reducing conditions (50 mM dithiothreitol (DTT)), on a 10% acrylamide gel, and was transferred onto a nitrocellulose membrane (Schleicher & Schuell, Dassel, Germany). The membrane was blocked with 5% skim milk (Tnuva, Rehovot, Israel) in Tris-buffered saline containing 0.05% Tween 20 (Sigma; TBST) for 1 h at room temperature. The membrane was then treated with the first antibody followed by peroxidase-conjugated second anti-

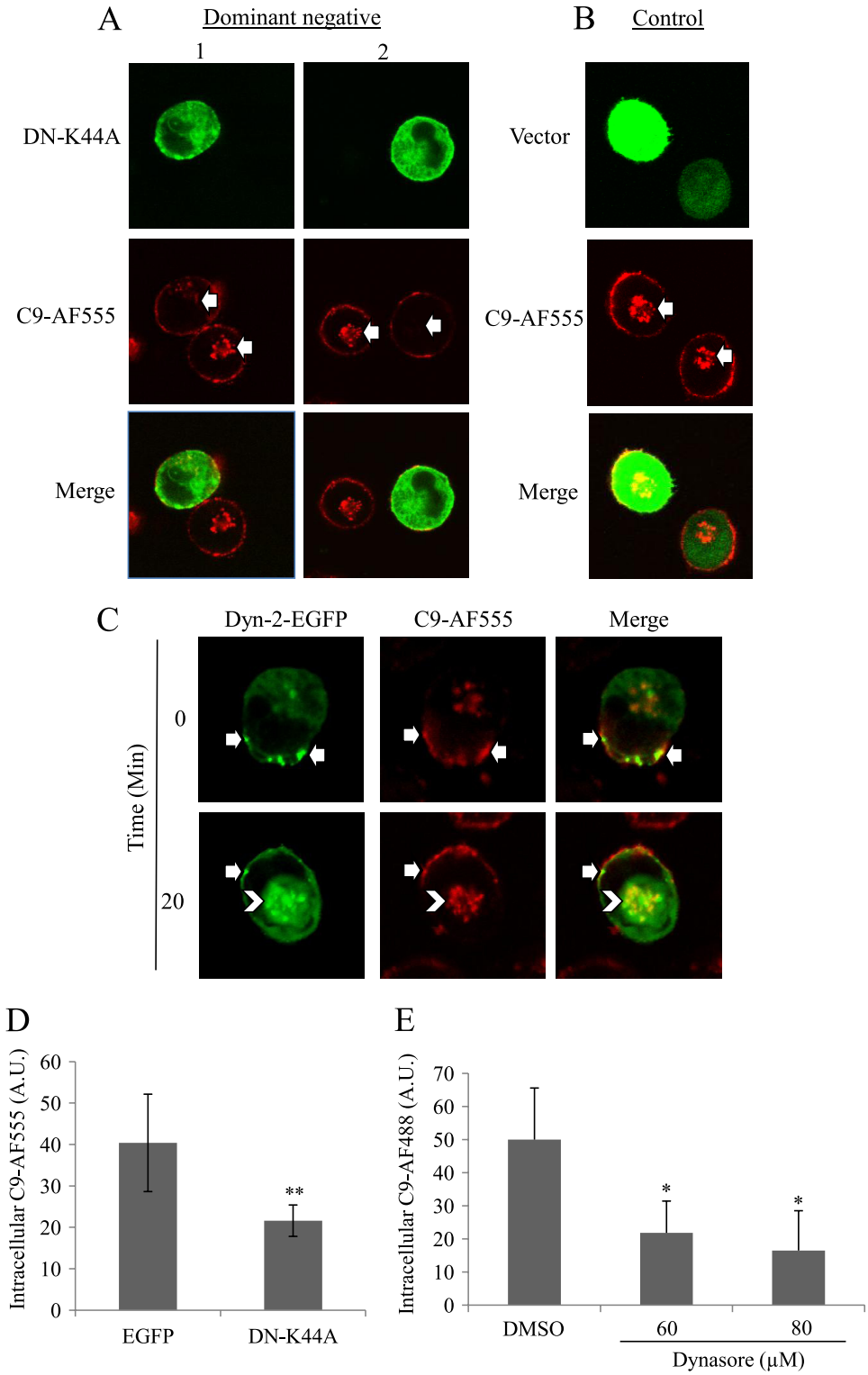

FIGURE 1. **Inhibition of dynamin abrogates MAC endocytosis.** K562 cells transfected with DN-K44A plasmid, Dyn-2-EGFP plasmid or with an empty vector (EGFP) as control were cultured for 48 h (*A*, *B*, *D*) or for 16 h (*C*). K562 cells were also pretreated with 0, 60, or 80 μM Dynasore for 30 min at 37 °C (*D–E*). Then, the cells were treated with a sublytic dose of anti-K562 antibodies and then with C9D-NHS supplemented with C9-AF555 (*A–D*) or C9-AF488 (*E*) for 10 min at 37 °C. Next, the cells were washed, incubated for 20 min at 37 °C and analyzed under a confocal microscope. Representative cells (four independent experiments) are shown. *White arrows* in pictures *A* and *B* point at C9-AF555 accumulating at the ERC. In *picture C*, *arrows* point to co-localized C9-AF555 and Dyn-2-EGFP at the cell membrane (*white arrows*) and at the ERC (*white arrowheads*). Levels of intracellular C9-AF555 (*D*) or C9-AF488 (*E*) were quantified in 50 randomly selected cell images by scanning with the Image J software (A.U.). Results are representative of four independent experiments. *, $p < 0.05$; **, $p < 0.01$.

body. Bands were developed with an enhanced chemiluminescence reagent (Pierce) and exposed to a SuperRX film (Fuji, Tokyo).

Tagging C9 with Alexa Fluor 488 or 555—C9 was tagged with the Alexa Fluor 488 or 555 dyes as described before (32). Briefly, purified human C9 (5 μg) was treated with the dye reagent

according to the manufacturer's instructions. The reagent mixture was stirred at room temperature for 60 min and the unbound dye was removed by using a spin column. The level of fluorescence of tagged C9-AF488 or 555 was analyzed in a Microplate Reader (Spectrafluor plus, Tecan, Austria).

Analysis of C3 and C5b-9 Deposition and Complement Regulators by Flow Cytometry—K562 cells were pretreated with 0, 2 or 5 mM methyl-β-cyclodextrin (MβCD), washed, and incubated with anti-K562 antiserum for 30 min at 4 °C and then with 50% C8D or HIS-C8D (for C3 deposition) or with 50% NHS or HIS (for C5b-9 deposition) for 10 min at 37 °C. Next, the cells were washed and fixed with 1% paraformaldehyde for 15 min at 4 °C. Next, cells were washed, labeled with goat anti-human C3 or mouse anti-neo C5b-9 (clone aE11) antibodies and a second FITC-labeled antibody, and analyzed in a FACScan (Becton Dickinson, San Jose). The results (7,000 cells) were analyzed with WinMDI 2.8 and mean fluorescence intensity (MFI, G-mean) values were determined. As controls, cells were treated with the second antibody alone. To measure the level of the complement regulatory proteins CD59 or CD55, K562 cells treated or not with MβCD and labeled with mouse anti-CD59 or anti-CD55 antibodies, respectively, and a second FITC-labeled antibody.

Imaging by Confocal Microscopy—Transfected or non-transfected cells were treated with antibody and NHS, HIS, or C9D-NHS supplemented with C9-AF488 or C9-AF555 for 10 min at 37 °C. Next, cells were washed and incubated at 37 °C for different time points. In some experiments, the cells were fixed with 1% paraformaldehyde and either permeabilized with saponin or not and further immunolabeled. Cells were analyzed under a Zeiss Laser Scanning Confocal Microscope 510 (Oberkochen, Germany). Images and merged images were obtained with the LSM software (Carl Zeiss, Germany). Images were processed further for display by using Image J (NIH, Bethesda, MD). Minimal laser intensities were used for image collection to minimize risks of photobleaching or phototoxicity.

Analysis of Transferrin Endocytosis—Transfected or non-transfected cells were incubated with Texas Red-conjugated transferrin (Tfr-TR) in binding buffer (RPMI 1640, 20 mM Hepes, pH 7.4 and 1 mg/ml BSA) for 30 min at 4 °C, washed and further incubated at 37 °C for various times. After washing and fixation, the cells were analyzed under a confocal microscope as described above.

Statistical Analysis—Student's two-sided unpaired t-tests were used to determine the statistical significance of differences between various data sets. Results are expressed as arithmetic mean ± S.D. Statistical significance was assumed when $p < 0.05$.

RESULTS

MAC Endocytosis Is Dynamin-dependent—To examine the involvement of dynamin in MAC endocytosis, we transfected K562 cells with a dominant-negative interfering K44A plasmid (38) or with Dyn-2-EGFP. By replacing in human serum the native C9 with a C9-Alexa Fluor 555 (C9-AF555) or C9-Alexa Fluor 488 (C9-AF488) (see below), MAC endocytosis could be tracked in cells expressing different fluorescently-labeled proteins. Tagged-C9 was found to be fully cytolytic on K562 cells (supplemental Fig. S1) (32). Cells transfected with K44A-EGFP or Dyn-2-EGFP were washed, treated with anti-K562 antibodies, and then with C9D-NHS supplemented with C9-AF555 for 10 min at 37 °C. Next, the cells were incubated for 20 min in HBSS at 37 °C, and then analyzed under a confocal microscope. The level of intracellular C9-AF555 was compared between K44A-positive and negative cells and between K44A-positive cells and control EGFP-positive cells. K44A expressing cells had reduced level of intracellular MAC in comparison to negative cells (Fig. 1*A*) and to pEGFP-transfected cells (Fig. 1, *A*, *B*, and *D*). Cells transfected with Dyn-2-EGFP and treated with complement had first (0 min) vesicles labeled with both C9-AF555 and Dyn-2-EGFP at the plasma membrane and later (20 min) co-localized C9-AF555 and Dyn-2-EGFP at the endocytic recycling compartment (Fig. 1*C*). To further investigate the role of dynamin in MAC endocytosis we employed Dynasore, a dynamin inhibitor which specifically interferes with the dynamin GTPase activity (39). K562 cells were pretreated with 0, 60, or 80 μM Dynasore for 30 min at 37 °C, washed and treated with antibody and NHS containing C9-AF488 (or with Tfr-TR) and analyzed under a confocal microscope. Dynasore reduced C9 endocytosis. A 2.5-fold reduction in intracellular MAC was observed in Dynasore treated cells in comparison to control cells (Fig. 1*E*). supplemental Fig. S2*D* presents few cells

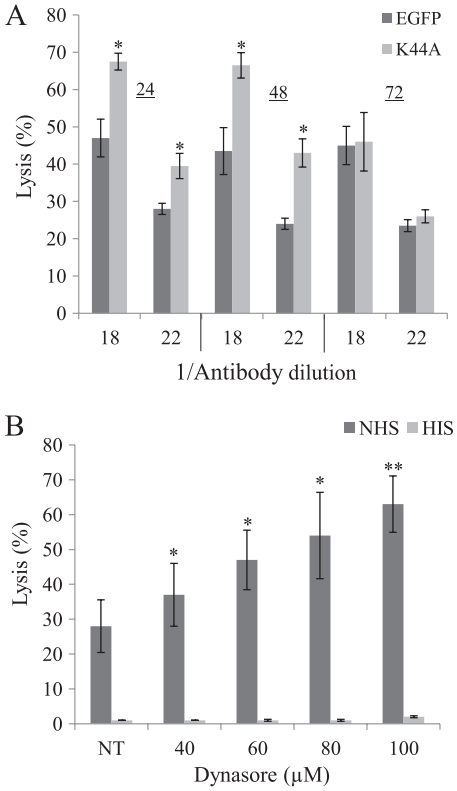

FIGURE 2. **Dynamin protects K562 cells from complement-dependent cytotoxicity.** K562 cells were transfected with the K44A plasmid or an empty vector control (EGFP) for 24, 48 or 72 h (*A*) or for 30 min at 37 °C with Dynasore at different concentrations (*B*). Then, the cells were subjected to treatment with an anti-K562 antiserum (diluted 1/18 or 1/22) followed by complement for 60 min at 37 °C. Cell lysis was determined by measuring uptake of trypan blue. Results are representative of four independent experiments, *, $p < 0.05$; **, $p < 0.01$.

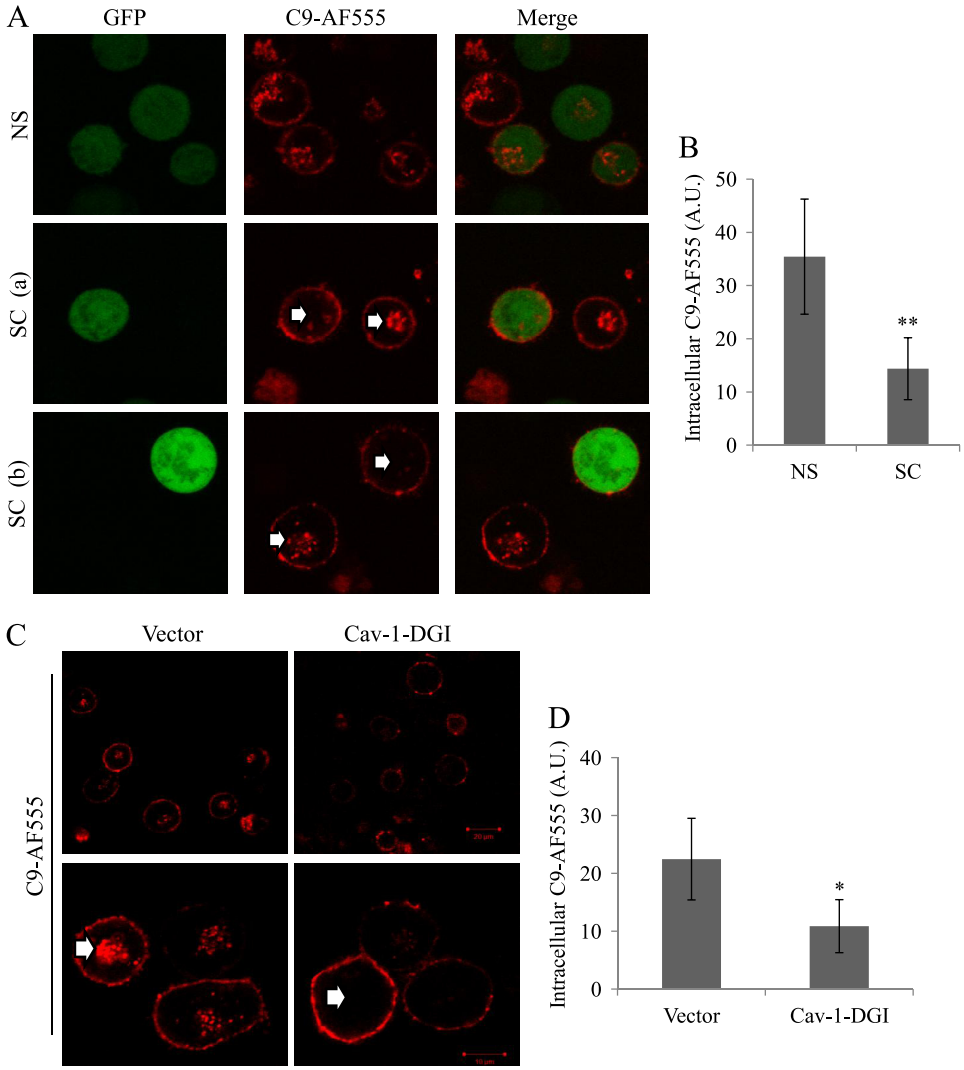

FIGURE 3. **Inhibition of Caveolin-1 abrogates MAC endocytosis.** *A* and *B*, K562 cells (10^7) were transfected for 48 h with 20 μg of Cav-1 shRNA (*SC*) or scrambled shRNA (*NS*) both mixed with 4 μg of pGFP. *C* and *D*, K562 cells (10^7) were transfected for 48 h with 18 μg of Cav-1-DGI plasmid or an empty vector as control. Transfected cells were treated with a sublytic dose of anti-K562 antibodies and then with C9D-NHS supplemented with C9-AF555 for 10 min at 37 °C. Next, the cells were washed, incubated for 20 min at 37 °C, and analyzed under a confocal microscope. *A* and *C*, representative fields are shown (three independent experiments). *White arrows* point to C9-AF555 accumulating in the ERC. Amount of endocytosed C9-AF555 was quantified in 50 randomly selected GFP-labeled cell images (*B*) or 50 randomly selected cell images (*D*) by using the Image J software (A.U.). Results are representative of three independent experiments, *, $p < 0.05$; **, $p < 0.01$.

treated or not with Dynasore and their level of C9-AF488 internalization. As expected, cells expressing K44A had reduced transferrin-Texas Red (Tfr-TR) uptake (supplemental Fig. S2, *A–C*) and cells treated with Dynasore also had lower uptake of Tfr-TR in comparison to control cells (supplemental Fig. S2, *E* and *F*).

Dynamin Is Essential for Protection Against CDC—To examine the significance of dynamin to complement resistance of K562 cells, K562 cells were transfected with the K44A plasmid or a control EGFP plasmid and after 24, 48, or 72 h were treated with anti-K562 antiserum (diluted 1/18 or 1/22) and then with complement (NHS) for 60 min at 37 °C. As shown in Fig. 2*A*, cells expressing K44A were significantly more sensitive to CDC in comparison to control cells. The decrease in the level of expression of the K44A plasmid after 72 h (data not shown) was accompanied by normalization of the cell sensitivity to CDC. Inhibition of dynamin with Dynasore prior to treatment of the cells with antibodies and complement sensitized the cells to CDC in a dose-dependent manner (Fig. 2*B*). As shown in cells treated with HIS, Dynasore had no toxic effect in the absence of complement (Fig. 2*B*).

MAC Endocytosis Depends on Caveolin-1—K562 cells express undetectable levels of Cav-1 and expression of recombinant Cav-1 in the cells was sufficient to reconstitute in them formation of caveolae (40). We observed that expression of Cav-1-EGFP in K562 cells resulted in a marked up-regulation of endogenous Cav-1 expression (supplemental Fig. S3*A*). The effect of Cav-1 silencing with shRNA on MAC endocytosis was examined in K562 cells that were first transfected with Cav-1-EGFP or with an empty vector as control. After 48 h the transfectants were further transfected with Cav-1 shRNA (SC) or scrambled shRNA (NS). First, cell lysates were prepared after 48 h and analyzed by Western blotting with anti-caveolin-1 and anti-actin antibodies. Cav-1 shRNA specifically reduced

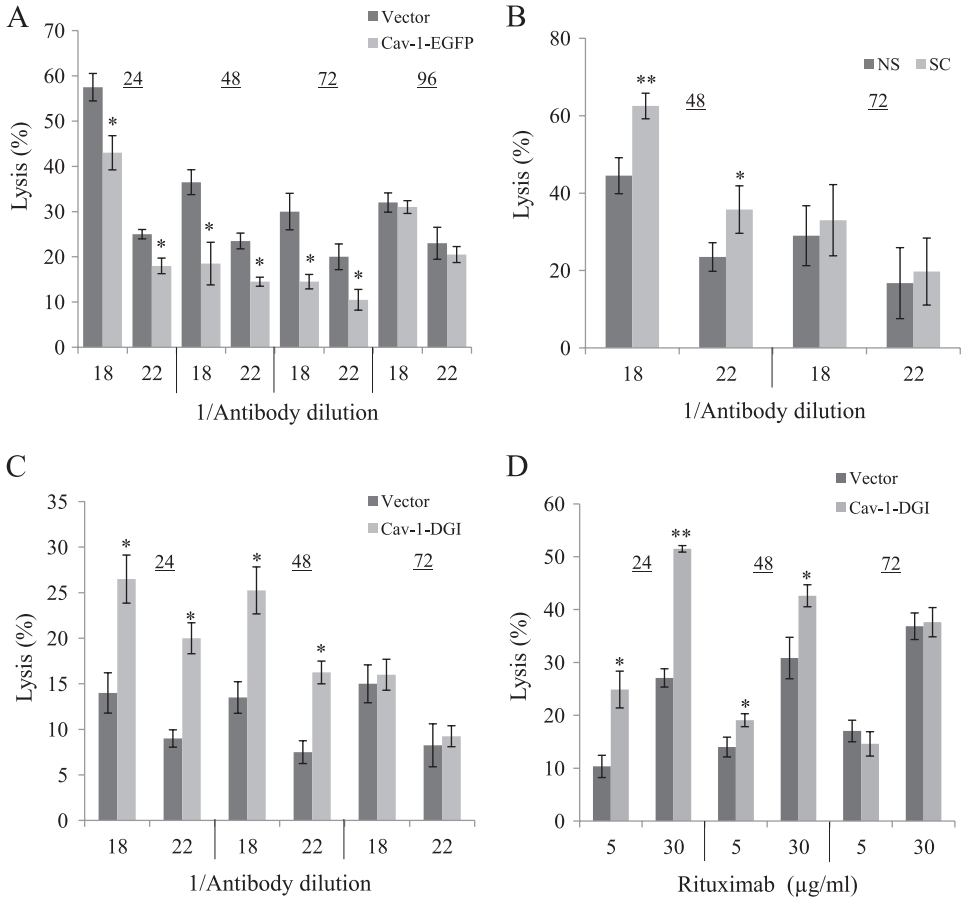

FIGURE 4. **Caveolin-1 protects K562 and Raji cells from complement-dependent cytotoxicity.** *A* and *B*, K562 cells (10^7) were transfected with 20 μg of Cav-1-EGFP plasmid or pEGFP as control or with 20 μg of Cav-1 shRNA (*SC*) or scrambled shRNA (*NS*) both mixed with 4 μg pGFP. *C* and *D*, K562 cells (*C*) or Raji cells (*D*) (10^7) were transfected with 18 μg of Cav-1-DGI or with pcDNA3.1 as control. After 24, 48, 72, or 96 h the cells were treated with anti-K562 antiserum (diluted 1/18 or 1/22) (*A–C*) or with Rituximab (5 or 30 μg/ml) (*D*) and then with NHS, for 60 min at 37 °C. Cell lysis was determined by measuring uptake of trypan blue. Results are representative of four independent experiments, *, $p < 0.05$; **, $p < 0.01$.

expression of endogenous Cav-1 by more than 90% relative to control shRNA (supplemental Fig. S3*B*). Next, cells were transfected with shRNA premixed with pGFP. The GFP served as an indicator of successful transfection. These cells were also subjected to treatment with anti-K562 antibodies and complement (C9D-NHS supplemented with C9-AF555) and were analyzed under a confocal microscope. Fig. 3*A* shows in red the distribution of MAC in the cells, some of it was on the cell surface and some in the endosomal recycling compartment (ERC). Cells transfected with control shRNA showed a considerable amount of the MAC accumulating within the cells in the ERC. In contrast, cells transfected with Cav-1 shRNA (labeled with GFP) expressed most of the MAC on their cell surface. Quantification of the amount of MAC in the ERC indicated a ~2.5-fold reduction in intracellular MAC accumulation in Cav-1 shRNA transfectants in comparison to SC transfectants (Fig. 3*B*). To further investigate the role of Cav-1 in MAC endocytosis, K562 cells were transfected with the dominant interfering Cav-1-DGI (36). After 48 h, the cells were treated with anti-K562 antibodies and then with C9D-NHS supplemented with C9-AF555 and analyzed under a confocal microscope. As demonstrated in Figs. 3*C*, D, Cav-1-DGI expressing cells failed to endocytose the MAC relative to control cells expressing an empty vector. Inhibition of dynamin-2 with Dynasore had a similar inhibitory effect on MAC endocytosis in Cav-1-DGI expressing and control cells (data not shown). Cav-1 silencing or inhibition had no effect on clathrin-mediated endocytosis of Tfr-TR (supplemental Fig. S4).

Caveolin-1 Is Essential for Protection from CDC—To examine the significance of Cav-1 to cell protection against CDC, the effects of Cav-1 up-regulation, silencing, or inhibition on lysis of K562 or Raji cells by complement were tested. Elevated expression of Cav-1 in K562 cells transfected with Cav-1-EGFP led to a lower sensitivity to CDC (Fig. 4*A*). In contrast, cells transfected with Cav-1 shRNA were more sensitive to CDC than cells transfected with control shRNA (Fig. 4*B*). Similarly, transfection with a Cav-1-DGI plasmid enhanced CDC of K562 and Raji cells relative to cells transfected with an empty vector (Fig. 4, *C* and *D*). The sensitizing effects of Cav-1 shRNA and Cav-1-DGI reached a peak at 48 h and faded away after 72 h. The protective effect of Cav-1-EGFP transfection lasted for 3 days and disappeared on day 4.

MAC Co-localizes with Cav-1 during Endocytosis—To further investigate the role of Cav-1 in MAC endocytosis, Cav-1-EGFP expressing cells were treated with anti-K562 antibodies and then with C9D-NHS supplemented with C9-AF555 and the cells were analyzed under a confocal microscope (Fig. 5, *A* and *B*). Intracellular vesicles labeled with both C9-AF555 and Cav-

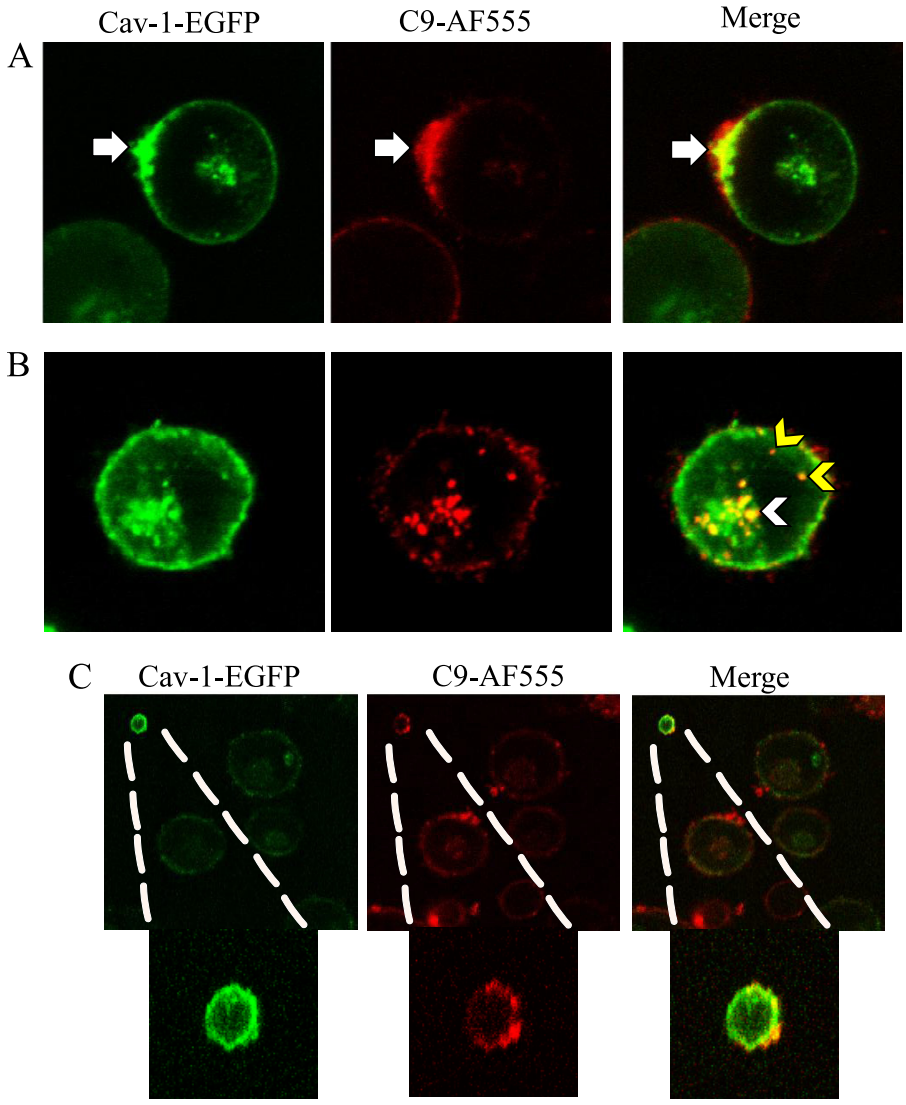

FIGURE 5. **Co-localization of the MAC with Cav-1-EGFP.** K562 cells were transfected with Cav-1-EGFP. After 48 h, the cells were treated with a sublytic dose of anti-K562 antibodies and then with C9D-NHS supplemented with C9-AF555 for 10 min at 37 °C. Next, the cells were washed (*A*) or further incubated for 20 min at 37 °C (*B*) and analyzed under a confocal microscope. Representative cells of three independent experiments are shown. *Arrows* point to co-localization of C9-AF555 and Cav-1-EGFP at the cell membrane (*white arrows*), the early endosome compartment (*yellow arrowheads*) and at the ERC (*white arrowheads*). *C*, an extracellular vesicle containing both Cav-1-EGFP and C9-AF555 is shown.

1-EGFP, were observed at the plasma membrane (caveolae), at the cell periphery (early endosomal compartment) and in the ERC. Apparently, the cells transported the endocytosed MAC complexes from the plasma membrane via endosomes to the ERC region. Extracellular vesicles labeled with both C9-AF555 and Cav-1-EGFP, were also seen (Fig. 5*C*) suggesting that Cav-1 may also be involved in exo-vesiculation of the MAC.

Exo-vesiculation of the MAC Is Cav-1-dependent—To further investigate the role of Cav-1 in exo-vesiculation of the MAC, the amount of C9 released from cells transfected with Cav-1-EGFP or Cav-1-DGI plasmid or an empty plasmid was compared. Transfectants were treated with antibody and NHS and washed and at different times of incubation at 37 °C supernatants were collected and analyzed by Western blotting with anti-C9 antibodies. As shown in Fig. 6, Cav-1-DGI suppressed the release of C9. In contrast, Cav-1-EGFP expressing cells released C9 at a faster rate.

Extent of MAC Deposition on K562 Cells Is Inversely Related to the Amount of Caveolin-1—Our earlier findings demonstrated that at the single cell level K562 cells show a large variability in complement activation and amount of deposited MAC (32). A correlation between the expression level of Cav-1 and the deposition of MAC was sought. Cav-1-EGFP-expressing cells were treated with anti-K562 antibodies and then with C9D-NHS supplemented with C9-AF555. The cells were then washed, fixed, and examined under a confocal microscope and the quantity of C9-AF555 and Cav-1-EGFP on single cells was examined. As shown in Fig. 7, *A* and *B*, cells expressing high levels of Cav-1 deposited lower levels of MAC. This inverse correlation was found to be statistically significant (Fig. 7*C*). A similar analysis was performed to correlate the amount of EGFP in cells transfected with an empty vector with the level of MAC deposition. No correlation was found between MAC deposition and EGFP content in the cells (Fig. 7*D*). To exclude the possi-

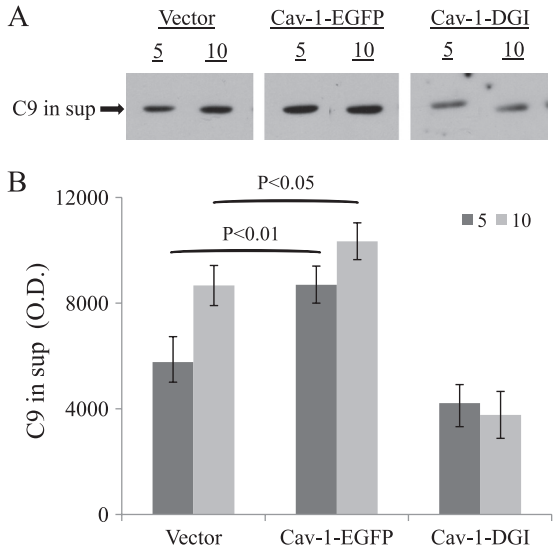

FIGURE 6. **Caveolin-1 contributes to MAC elimination by exo-vesiculation.** K562 cells were transfected with a Cav-1-EGFP or Cav-1-DGI plasmid or with an empty vector as control. After 48 h the cells were treated with a sublytic dose of anti-K562 antiserum and then with NHS for 10 min at 37 °C. The cells were extensively washed with HBSS and incubated at 37 °C for 5 or 10 min. The cell supernatant (*sup*) was collected and cleared by centrifugation at 5,000 × *g*, subjected to SDS-PAGE and analyzed by Western blotting with anti-C9 antibodies. *A*, representative C9 protein bands in sup. *B*, results of densitometric analyses of protein bands from three independent experiments.

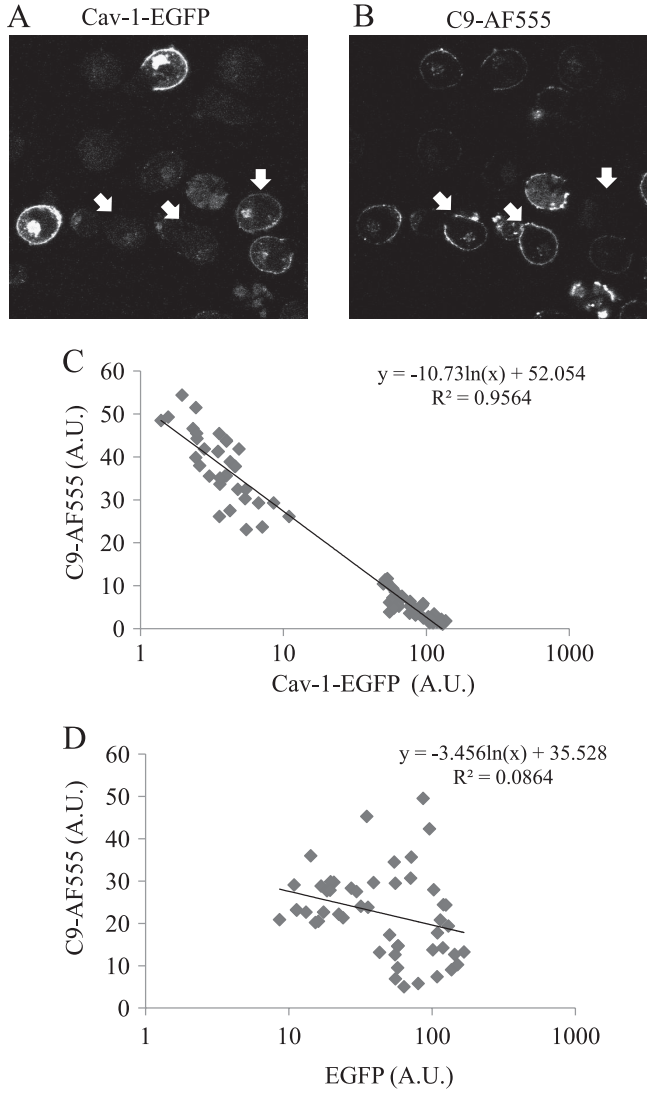

FIGURE 7. **MAC deposition is inversely correlated with the level of Cav-1-EGFP expression.** *A* and *B*, K562 cells were transfected with Cav-1-EGFP plasmid or EGFP plasmid as control. After 48 h, the cells were treated with a sublytic dose of anti-K562 antibodies and then with C9D-NHS supplemented with C9-AF555 for 10 min at 37 °C. Next, the cells were washed and analyzed under a confocal microscope. A selected image representing numerous similar images is shown in *A* and *B*. *White arrows* point at 3 cells showing low levels of Cav-1-EGFP and high levels of C9-AF555. *C* and *D*, amounts of C9-AF555 and Cav-1-EGFP or EGFP (A.U.) were quantified with the Image J software in 80 randomly selected cell images. *C*, a significant inverse correlation is shown between the quantities of C9-AF555 and Cav-1-EGFP ($R^2 = 0.9564$; $p < 0.05$). *D*, no correlation is seen between the levels of C9-AF555 and EGFP ($R^2 = 0.0864$).

bility that Cav-1-EGFP expression is affecting or correlated with the amount of surface CD59 molecules, the level of CD59 on Cav-1-EGFP expressing K562 cells was similarly analyzed. There was no correlation at the single cells level between Cav-1-EGFP and CD59 expression (supplemental Fig. S5).

Lipid Rafts Are Involved in Protection from CDC and in MAC Endocytosis—Caveolae are considered one form of membrane lipid rafts (26). To examine the involvement of lipid rafts in protection from CDC and in MAC endocytosis, K562 cells were treated with two membrane cholesterol depletion agents, methyl-β-cyclodextrin (MβCD), or filipin III, and then subjected to complement-dependent cytotoxicity. As shown in Fig. 8, *A* and *B*, treatment with MβCD (more than 2 mM) or filipin III (more than 12 μM) significantly sensitized, in a dose-dependent manner, K562 cells to CDC. Using the cholesterol repletion assay, cells pretreated with MβCD or untreated cells were washed and treated with 0, 1, 2, or 4 mM cholesterol for 15 min at 37 °C. Then, the cells were treated with anti-K562 antibodies and NHS for 60 min at 37 °C. Cholesterol repletion reversed the sensitizing effect of MβCD on CDC (Fig. 8*C*). Furthermore, enrichment of membrane cholesterol in control cells significantly reduced lysis of K562 cells by complement (Fig. 8*C*).

Streptolysin O (SLO) is a pore-forming protein that uses cholesterol as a receptor for its membrane insertion and activation of cell death (41). To validate that MβCD treatment disrupted membrane cholesterol in K562 cells, we examined the effect of MβCD on SLO-mediated cell lysis. K562 cells were first incubated with MβCD, washed and then incubated with SLO (activated with DTT) or DTT alone for 30 min at 37 °C. As shown in Fig. 8*D*, pretreatment with MβCD abolished SLO-mediated lysis.

The enhancing effect of MβCD on CDC could be the result of increased C3 and C5b-9 deposition on the cells and/or reduction in the level of expression of the membrane complement regulators CD55 or CD59 that have a GPI-anchor. K562 cells were treated with MβCD and then subjected to treatment with anti-K562 antibodies and complement and the amount of deposited C3 and C5b-9 was quantified. In addition, the effect of MβCD treatment on expression of CD55 and CD59 was tested. MβCD treatment had neither effect on C3 or C5b-9 deposition nor on CD55 and CD59 expression (supplemental Fig. S6). Then, the effect of MβCD on MAC endocytosis was tested. K562 cells treated with MβCD lost their capacity to internalize the MAC complexes (Fig. 8*E*).

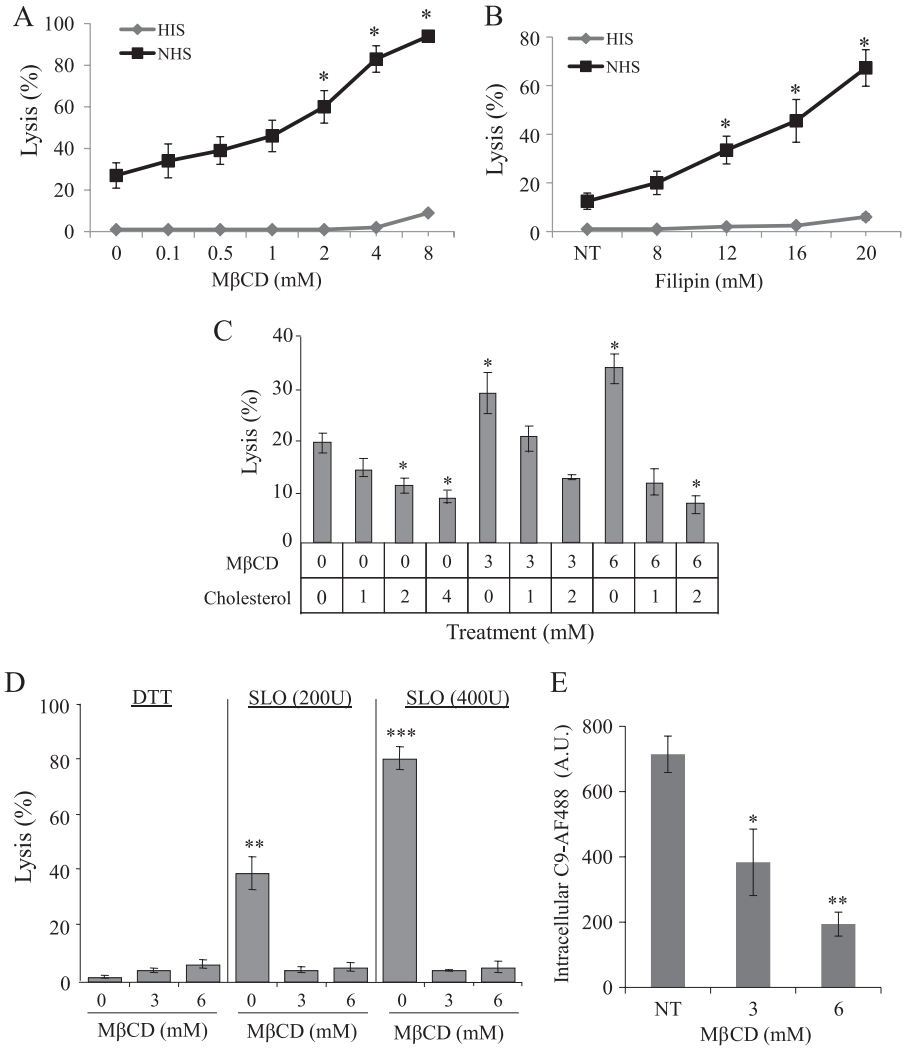

FIGURE 8. **Cholesterol depletion sensitizes cells to complement-mediated lysis but protects from SLO-mediated lysis.** K562 cells were pretreated with the indicated doses of MβCD (*A*, *C*, *D*) for 15 min or filipin-III (*B*) for 30 min at 37 °C. For cholesterol repletion (*C*), cells were first incubated with MβCD and then washed and treated with 0, 1, 2, or 4 mM cholesterol for 15 min at 37 °C. Cell lysis was activated by treatment with a sublytic dose of anti-K562 antibodies and NHS (or HIS as control) for 60 min at 37 °C. *D*, cells were first incubated with 0, 3, or 6 mM MβCD, washed and incubated with 200 or 400 units of SLO in DTT or DTT alone (0.4 mM) as control, for 30 min at 37 °C. Cell lysis was determined by trypan blue uptake. All results are representative of four independent experiments. *E*, K562 cells were pretreated with 0, 3 or 6 mM of MβCD for 15 min at 37 °C. Then, the cells were treated with a sublytic dose of anti-K562 antibodies and C9D-NHS supplemented with C9-AF488 for 10 min at 37 °C. Next, the cells were washed, incubated for 20 min at 37 °C, and analyzed under a confocal microscope. The amount of intracellular C9-AF488 was quantified with the Zeiss 410 LSM software in 100 randomly selected cell images (Relative fluorescence intensity; R.F.I.). *, $p < 0.05$; **, $p < 0.01$; ***, $p < 0.001$.

Clathrin Is Not Involved in CDC and in MAC Endocytosis—A possible role for clathrin in CDC and MAC endocytosis was first examined by RNAi-mediated suppression of the clathrin heavy chain (CHC). K562 cells were transfected with a specific shRNA directed to CHC or a scrambled shRNA, mixed with pGFP (served as a marker of transfectants). Transfection with CHC shRNA reduced after 72 h the expression of endogenous CHC by ~80% relative to control (supplemental Fig. S7*A*). After addition of Tfr-TR to these cells, we observed a marked reduction in entry of Tfr-TR into cells transfected with CHC shRNA relative to control cells transfected with scrambled shRNA (supplemental Fig. S7, *B* and *C*).

Next, we tested whether cell sensitivity to CDC and MAC endocytosis are affected or not by silencing of the CHC. As presented in Fig. 9, K562 cells transfected with CHC shRNA or scrambled shRNA showed the same sensitivity to complement-mediated lysis (Fig. 9*A*) and the same amount of intracellular C9 (Fig. 9, *C* and *D*). Another approach to inhibit clathrin-mediated endocytosis is by using a dominant interfering epidermal growth factor receptor substrate 15 (DN-EPS15) (42). EPS15, a component of the clathrin-coated pit is constitutively associates with Adaptor Protein-2 (AP-2) and is required for its docking onto the plasma membrane. DN-EPS15 is unable to bind AP-2 and inhibits clathrin-coated pit formation (42). K562 cells were transfected with DN-EPS15 plasmid or control GFP plasmid. As expected, uptake of Tfr-TR into DN-EPS15 transfectants was reduced relative to control cells (supplemental Fig. S8, *A* and *B*). In contrast, cell sensitivity to CDC and MAC endocytosis were not affected by DN-EPS15 (Fig. 9, *B* and *E* and supplemental Fig. S8*C*).

DISCUSSION

Within minutes after a sublytic complement attack, K562 cells release membrane vesicles loaded with the MAC/C5b-9

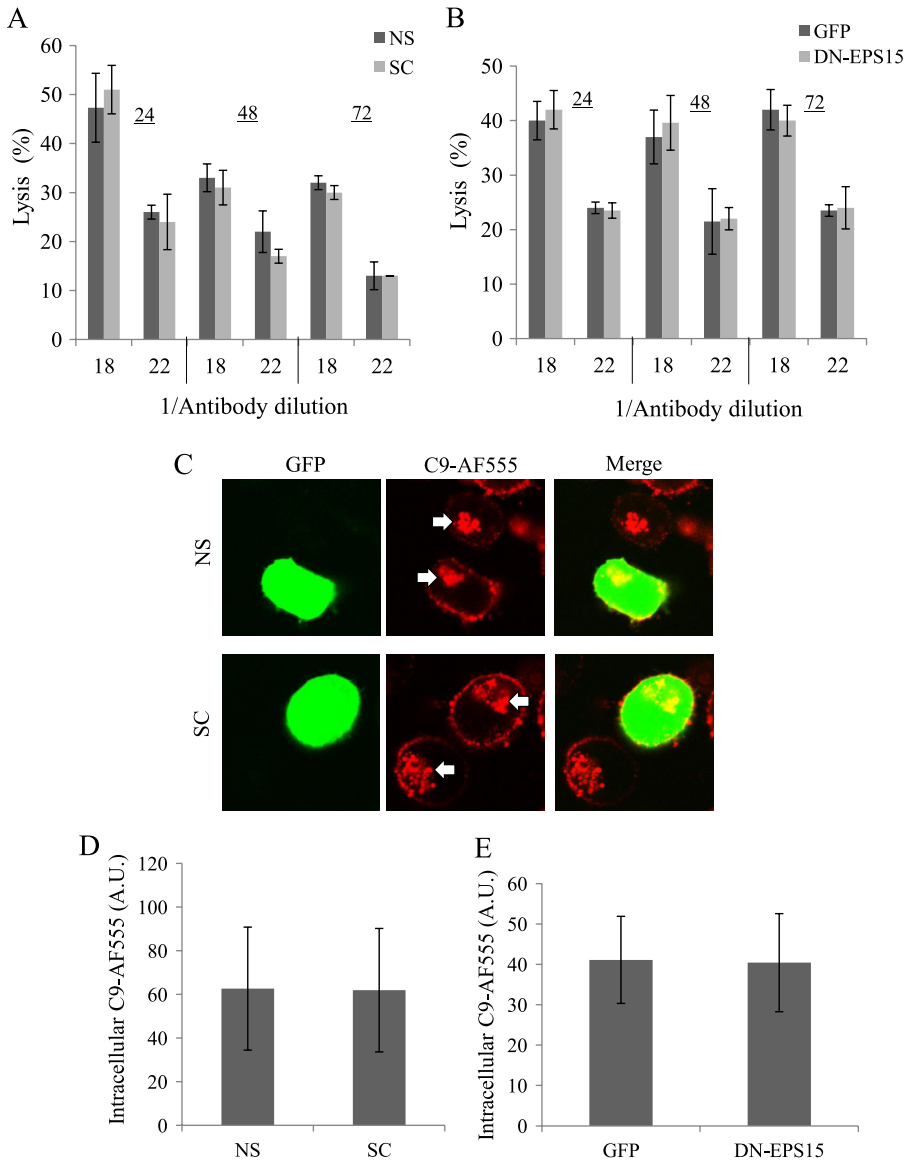

FIGURE 9. **Inhibition of clathrin-mediated endocytosis has no effect on complement-dependent cytotoxicity and on MAC endocytosis.** *A*, *C*, and *D*, K562 cells were transfected with specific shRNA directed to CHC (*SC*) or with a nonspecific shRNA (*NS*). *B* and *E*, K562 cells were transfected with a plasmid containing the dominant negative epidermal growth factor receptor substrate 15 (DN-EPS15) or with an empty GFP plasmid. *A* and *B*, after 24, 48, or 72 h, the cells were treated with anti-K562 antiserum (diluted 1/18 or 1/22) and then with NHS for 60 min at 37 °C. Cell lysis was determined by measuring uptake of trypan blue. *C–E*, 72 h (*C* and *D*) or 24 h (*E*) post-transfection the cells were treated with a sublytic dose of anti-K562 antibodies and then with C9D-NHS supplemented with C9-AF555 for 10 min at 37 °C. Next, the cells were washed, incubated for 20 min at 37 °C, and analyzed under a confocal microscope. Representative cells (of four independent experiments) are shown in *C*; *arrows* point at a C9-AF555 accumulation in the ERC. *D* and *E*, amount of intracellular C9-AF555 was quantified with the Image J software in 50 randomly selected cell images.

complexes and few minutes later, internalize C5b-9 complexes through the endocytic machinery and accumulate it in the ERC (32). Internalized C5b-9 complexes may be either packed within the multivesicular bodies and transported for exocytosis or subjected to proteolytic degradation. The molecular mechanism controlling MAC endocytosis is still largely unknown. The purpose of this study was to get a deeper insight into the MAC endocytic pathway and to test the hypothesis that it serves as a rescue mechanism against CDC. Our findings demonstrate that specific inhibition of clathrin-mediated endocytosis either by knocking down of the clathrin heavy chain with shRNA or with the dominant interfering DN-EPS15, conditions shown to abrogate transferrin endocytosis, no effect on CDC or MAC endocytosis was observed (Fig. 9 and supplemental Figs. S7 and S8). Hence, we conclude that the MAC endocytic mechanism is clathrin-independent. We then examined the involvement of the large GTPase Dynamin in MAC endocytosis. Dynamin facilitates fission of endocytic vesicles and is essential for endocytosis (23). Mammals express three Dynamin genes Dyn-1, Dyn-2, and Dyn-3. Dyn-2 is expressed in most cell types whereas Dyn-1 and Dyn-3 are tissue specific (43). To inhibit Dynamin-2 activity we treated the cells with the dominant interfering K44A dynamin (38) or with Dynasore, a general Dynamin inhibitor which specifically interferes with the GTPase activity of Dynamin (39). As expected, both treatments abrogated transferrin endocytosis (supplemental Fig. S2). More interestingly, Dynamin-2 was found to be

important for MAC internalization and for cell protection from CDC (Figs. 1 and 2).

Dynamin is also involved in the clathrin-independent pathway that is mediated by caveolae (24, 25). Caveolae are plasma membrane invaginations in which the major constituent Cav-1 functions as a principal structural component (27, 29). To examine the possible involvement of Cav-1 in MAC endocytosis we inhibited Cav-1 either by blocking Cav-1 synthesis with a Cav-1 specific shRNA or by using the dominant interfering Cav-1-DGI (37). Both treatments sensitized cells to CDC and inhibited MAC endocytosis (Figs. 3 and 4). In contrast, overexpression of Cav-1 protected the cells from CDC (Fig. 4). An inverse linear correlation is seen between the level of Cav-1 overexpression and the amount of C5b-9 deposition following complement activation (Fig. 7). Furthermore, Cav-1-EGFP co-localized with MAC in the plasma membrane, early endosomes and the ERC (Fig. 5). The results indicate that Dyn-2 and Cav-1 (but not clathrin) support cell resistance to CDC, probably by targeting the MAC to a clathrin-independent, caveolae-mediated endocytic clearance pathway.

Caveolae are one form of membrane lipid rafts. Our data suggest that lipid rafts integrity is essential for cell resistance to CDC, thus disruption of membrane cholesterol with MβCD or Filipin III abolished resistance to CDC and inhibited MAC endocytosis (Fig. 8 and supplemental Fig. S7). Hayer *et al.* demonstrated that caveolae bud from the plasma membrane carrying Cav-1 to the early endosome (44). However, cholesterol disruption causes disassembly of caveolae, endocytosis of Cav-1 as a cargo protein, caveolin ubiquitination, and accumulation of Cav-1 in the internal membranes of late endosomes. This results in accelerated degradation of Cav-1 (44). It is conceivable that cholesterol disruption lead to Cav-1 degradation, dissolution of caveolae, reduced MAC endocytosis or exo-vesiculation and eventually increased cell sensitivity to CDC. Since the dynamin and cholesterol inhibitors interfered with MAC elimination in K562 cells which express low Cav-1 level, it is possible that a caveolae-independent, dynamin- and cholesterol-dependent endocytic pathway is also involved in MAC removal (45). This possibility awaits further examination.

K562 cells eliminate the MAC by endocytosis but also by exo-vesiculation (32). In order to examine the possible involvement of Cav-1 in MAC exo-vesiculation, we inhibited Cav-1 by using the dominant interfering Cav-1-DGI or over-expressed Cav-1. Inhibition of Cav-1 abrogated the amount of secreted C5b-9, whereas, overexpression of Cav-1 increased C5b-9 exo-vesiculation (Fig. 6). In addition, cholesterol disruption by MβCD dramatically inhibited C9 exo-vesiculation (data not shown). These findings suggest that Cav-1 (and probably caveolae) is also involved in MAC exo-vesiculation. The molecular mechanism of MAC internalization, exo-vesiculation and resistance to CDC via a Cav-1-dependent pathway needs to be further investigated. Interestingly, caveolae can also bypass the sorting organelles and directly fuse back with the plasma membrane in a kiss-and-run manner, a process regulated by protein kinases (46). It is possible that this short-range traffic of caveolae facilitates interaction of the MAC with caveolae and its exo-vesiculation. This could be related to our observation of co-localization of MAC and Cav-1 in the vicinity of the plasma membrane and on exo-vesicles (Fig. 5). Cav-1 is differentially over-expressed in cancer cells (47–49) and it increases the resistance of tumor cells to drug-induced apoptosis by a mechanism involving phosphorylation of PKCα (50). Cav-1-dependent internalization is involved in PKCϵ-mediated inhibition of vascular K(ATP) channels (51). PKC plays a role also in protection of K562 cells from CDC (52) and in MAC elimination (19, 32). It is suggested that Cav-1 protection from CDC involves PKC or other protein kinases.

Acknowledgments—shRNA against Caveolin-1 and scrambled shRNA were kindly provided by Dr. Maria Shatz (NIEHS, NC).

REFERENCES

1. Walport, M. J. (2001) Complement. Second of two parts. *N. Engl. J. Med.* **344,** 1140–1144
2. Ricklin, D., Hajishengallis, G., Yang, K., and Lambris, J. D. (2010) Complement: a key system for immune surveillance and homeostasis. *Nat. Immunol.* **11,** 785–797
3. Müller-Eberhard, H. J. (1986) The membrane attack complex of complement. *Annu. Rev. Immunol.* **4,** 503–528
4. Fishelson, Z., Attali, G., and Mevorach, D. (2001) Complement and apoptosis. *Mol. Immunol.* **38,** 207–219
5. Papadimitriou, J. C., Drachenberg, C. B., Shin, M. L., and Trump, B. F. (1994) Ultrastructural studies of complement mediated cell death: a biological reaction model to plasma membrane injury. *Virchows Arch.* **424,** 677–685
6. Tschopp, J., Podack, E. R., and Müller-Eberhard, H. J. (1985) The membrane attack complex of complement: C5b-8 complex as accelerator of C9 polymerization. *J. Immunol.* **134,** 495–499
7. Ziporen, L., Donin, N., Shmushkovich, T., Gross, A., and Fishelson, Z. (2009) Programmed necrotic cell death induced by complement involves a Bid-dependent pathway. *J. Immunol.* **182,** 515–521
8. Gancz, D., Donin, N., and Fishelson, Z. (2009) Involvement of the c-jun N-terminal kinases JNK1 and JNK2 in complement-mediated cell death. *Mol. Immunol.* **47,** 310–317
9. Carney, D. F., Koski, C. L., and Shin, M. L. (1985) Elimination of terminal complement intermediates from the plasma membrane of nucleated cells: the rate of disappearance differs for cells carrying C5b-7 or C5b-8 or a mixture of C5b-8 with a limited number of C5b-9. *J. Immunol.* **134,** 1804–1809
10. Scolding, N. J., Morgan, B. P., Houston, W. A., Linington, C., Campbell, A. K., and Compston, D. A. (1989) Vesicular removal by oligodendrocytes of membrane attack complexes formed by activated complement. *Nature* **339,** 620–622
11. Sims, P. J., and Wiedmer, T. (1986) Repolarization of the membrane potential of blood platelets after complement damage: evidence for a Ca^{2+}-dependent exocytotic elimination of C5b-9 pores. *Blood* **68,** 556–561
12. Stein, J. M., and Luzio, J. P. (1991) Ectocytosis caused by sublytic autologous complement attack on human neutrophils. The sorting of endogenous plasma-membrane proteins and lipids into shed vesicles. *Biochem. J.* **274,** 381–386
13. Donin, N., Jurianz, K., Ziporen, L., Schultz, S., Kirschfink, M., and Fishelson, Z. (2003) Complement resistance of human carcinoma cells depends on membrane regulatory proteins, protein kinases and sialic acid. *Clin. Exp. Immunol.* **131,** 254–263
14. Jurianz, K., Ziegler, S., Donin, N., Reiter, Y., Fishelson, Z., and Kirschfink, M. (2001) K562 erythroleukemic cells are equipped with multiple mechanisms of resistance to lysis by complement. *Int. J. Cancer* **93,** 848–854
15. Varsano, S., Frolkis, I., Rashkovsky, L., Ophir, D., and Fishelson, Z. (1996) Protection of human nasal respiratory epithelium from complement-mediated lysis by cell-membrane regulators of complement activation. *Am. J. Respir. Cell Mol. Biol.* **15,** 731–737
16. Kerjaschki, D., Schulze, M., Binder, S., Kain, R., Ojha, P. P., Susani, M.,

Horvat, R., Baker, P. J., and Couser, W. G. (1989) Transcellular transport and membrane insertion of the C5b-9 membrane attack complex of complement by glomerular epithelial cells in experimental membranous nephropathy. *J. Immunol.* **143,** 546–552
17. Morgan, B. P., Dankert, J. R., and Esser, A. F. (1987) Recovery of human neutrophils from complement attack: removal of the membrane attack complex by endocytosis and exocytosis. *J. Immunol.* **138,** 246–253
18. Morgan, B. P., Imagawa, D. K., Dankert, J. R., and Ramm, L. E. (1986) Complement lysis of U937, a nucleated mammalian cell line in the absence of C9: effect of C9 on C5b-8 mediated cell lysis. *J. Immunol.* **136,** 3402–3406
19. Pilzer, D., and Fishelson, Z. (2005) Mortalin/GRP75 promotes release of membrane vesicles from immune attacked cells and protection from complement-mediated lysis. *Int. Immunol.* **17,** 1239–1248
20. Pilzer, D., Saar, M., Koya, K., and Fishelson, Z. (2010) Mortalin inhibitors sensitize K562 leukemia cells to complement-dependent cytotoxicity. *Int. J. Cancer* **126,** 1428–1435
21. Mukherjee, S., Ghosh, R. N., and Maxfield, F. R. (1997) Endocytosis. *Physiol. Rev.* **77,** 759–803
22. Schmid, E. M., and McMahon, H. T. (2007) Integrating molecular and network biology to decode endocytosis. *Nature* **448,** 883–888
23. Bashkirov, P. V., Akimov, S. A., Evseev, A. I., Schmid, S. L., Zimmerberg, J., and Frolov, V. A. (2008) GTPase cycle of dynamin is coupled to membrane squeeze and release, leading to spontaneous fission. *Cell* **135,** 1276–1286
24. Henley, J. R., Krueger, E. W., Oswald, B. J., and McNiven, M. A. (1998) Dynamin-mediated internalization of caveolae. *J. Cell Biol.* **141,** 85–99
25. Oh, P., McIntosh, D. P., and Schnitzer, J. E. (1998) Dynamin at the neck of caveolae mediates their budding to form transport vesicles by GTP-driven fission from the plasma membrane of endothelium. *J. Cell Biol.* **141,** 101–114
26. Hansen, C. G., and Nichols, B. J. (2009) Molecular mechanisms of clathrin-independent endocytosis. *J. Cell Sci.* **122,** 1713–1721
27. Parton, R. G., and Simons, K. (2007) The multiple faces of caveolae. *Nat. Rev. Mol. Cell Biol.* **8,** 185–194
28. Williams, T. M., and Lisanti, M. P. (2004) The caveolin proteins. *Genome Biol.* **5,** 214
29. Rothberg, K. G., Heuser, J. E., Donzell, W. C., Ying, Y. S., Glenney, J. R., and Anderson, R. G. (1992) Caveolin, a protein component of caveolae membrane coats. *Cell* **68,** 673–682
30. Bauer, M., and Pelkmans, L. (2006) A new paradigm for membrane-organizing and -shaping scaffolds. *FEBS Lett.* **580,** 5559–5564
31. Mora, R., Bonilha, V. L., Marmorstein, A., Scherer, P. E., Brown, D., Lisanti, M. P., and Rodriguez-Boulan, E. (1999) Caveolin-2 localizes to the golgi complex but redistributes to plasma membrane, caveolae, and rafts when co-expressed with caveolin-1. *J. Biol. Chem.* **274,** 25708–25717
32. Moskovich, O., and Fishelson, Z. (2007) Live cell imaging of outward and inward vesiculation induced by the complement c5b-9 complex. *J. Biol. Chem.* **282,** 29977–29986
33. Schlesinger, M., Nave, Z., Levy, Y., Slater, P. E., and Fishelson, Z. (1990) Prevalence of hereditary properdin, C7 and C8 deficiencies in patients with meningococcal infections. *Clin. Exp. Immunol.* **81,** 423–427
34. Boll, W., Ehrlich, M., Collier, R. J., and Kirchhausen, T. (2004) Effects of dynamin inactivation on pathways of anthrax toxin uptake. *Eur. J. Cell Biol.* **83,** 281–288
35. Chetrit, D., Ziv, N., and Ehrlich, M. (2009) Dab2 regulates clathrin assembly and cell spreading. *Biochem. J.* **418,** 701–715
36. Massol, R. H., Larsen, J. E., Fujinaga, Y., Lencer, W. I., and Kirchhausen, T. (2004) Cholera toxin toxicity does not require functional Arf6- and dynamin-dependent endocytic pathways. *Mol. Biol. Cell* **15,** 3631–3641
37. Reiter, Y., Ciobotariu, A., and Fishelson, Z. (1992) Sublytic complement attack protects tumor cells from lytic doses of antibody and complement. *Eur. J. Immunol.* **22,** 1207–1213
38. Damke, H., Gossen, M., Freundlieb, S., Bujard, H., and Schmid, S. L. (1995) Tightly regulated and inducible expression of dominant interfering dynamin mutant in stably transformed HeLa cells. *Methods Enzymol.* **257,** 209–220
39. Kirchhausen, T., Macia, E., and Pelish, H. E. (2008) Use of dynasore, the small molecule inhibitor of dynamin, in the regulation of endocytosis. *Methods Enzymol.* **438,** 77–93
40. Parolini, I., Sargiacomo, M., Galbiati, F., Rizzo, G., Grignani, F., Engelman, J. A., Okamoto, T., Ikezu, T., Scherer, P. E., Mora, R., Rodriguez-Boulan, E., Peschle, C., and Lisanti, M. P. (1999) Expression of caveolin-1 is required for the transport of caveolin-2 to the plasma membrane. Retention of caveolin-2 at the level of the golgi complex. *J. Biol. Chem.* **274,** 25718–25725
41. Bhakdi, S., Tranum-Jensen, J., and Sziegoleit, A. (1985) Mechanism of membrane damage by streptolysin-O. *Infect. Immun.* **47,** 52–60
42. Benmerah, A., Lamaze, C., Bègue, B., Schmid, S. L., Dautry-Varsat, A., and Cerf-Bensussan, N. (1998) AP-2/Eps15 interaction is required for receptor-mediated endocytosis. *J. Cell Biol.* **140,** 1055–1062
43. Lajoie, P., and Nabi, I. R. (2010) Lipid rafts, caveolae, and their endocytosis. *Int. Rev. Cell Mol. Biol.* **282,** 135–163
44. Hayer, A., Stoeber, M., Ritz, D., Engel, S., Meyer, H. H., and Helenius, A. (2010) Caveolin-1 is ubiquitinated and targeted to intralumenal vesicles in endolysosomes for degradation. *J. Cell Biol.* **191,** 615–629
45. Mayor, S., and Pagano, R. E. (2007) Pathways of clathrin-independent endocytosis. *Nat. Rev. Mol. Cell Biol.* **8,** 603–612
46. Pelkmans, L., and Zerial, M. (2005) Kinase-regulated quantal assemblies and kiss-and-run recycling of caveolae. *Nature* **436,** 128–133
47. Ho, C. C., Kuo, S. H., Huang, P. H., Huang, H. Y., Yang, C. H., and Yang, P. C. (2008) Caveolin-1 expression is significantly associated with drug resistance and poor prognosis in advanced non-small cell lung cancer patients treated with gemcitabine-based chemotherapy. *Lung Cancer* **59,** 105–110
48. Lavie, Y., Fiucci, G., and Liscovitch, M. (1998) Up-regulation of caveolae and caveolar constituents in multidrug-resistant cancer cells. *J. Biol. Chem.* **273,** 32380–32383
49. Yang, C. P., Galbiati, F., Volonte, D., Horwitz, S. B., and Lisanti, M. P. (1998) Upregulation of caveolin-1 and caveolae organelles in Taxol-resistant A549 cells. *FEBS Lett.* **439,** 368–372
50. Tirado, O. M., MacCarthy, C. M., Fatima, N., Villar, J., Mateo-Lozano, S., and Notario, V. (2010) Caveolin-1 promotes resistance to chemotherapy-induced apoptosis in Ewing's sarcoma cells by modulating PKCα phosphorylation. *Int. J. Cancer* **126,** 426–436
51. Jiao, J., Garg, V., Yang, B., Elton, T. S., and Hu, K. (2008) Protein kinase C-ϵ induces caveolin-dependent internalization of vascular adenosine 5′-triphosphate-sensitive K^+ channels. *Hypertension* **52,** 499–506
52. Kraus, S., and Fishelson, Z. (2000) Cell desensitization by sublytic C5b-9 complexes and calcium ionophores depends on activation of protein kinase C. *Eur. J. Immunol.* **30,** 1272–1280